Int. J. Electrochem. Sci., 8 **(2013)** 6603 - 6609

International Journal of
ELECTROCHEMICAL
SCIENCE
www.electrochemsci.org

Synthesis and Characterization of $LiMnPO_4$ Nanoparticles Prepared by a Citric Acid Assisted Sol-Gel Method

S. Zhang[1,*], *F. L. Meng*[1], *Q. Wu*[1], *F. L. Liu*[1], *H. Gao*[1], *M. Zhang*[1], *C. Deng*[2,*]

[1] College of Material Science and Chemical Engineering, Harbin Engineering University, Harbin 150001, Heilongjiang, China
[2] Key Laboratory of Photonic and Electronic Bandgap Materials, Ministry of Education; College of Chemistry and Chemical Engineering, Harbin Normal University, Harbin, 150025, Heilongjiang, China
[*]E-mail: senzhang@hrbeu.edu.cn; chaodeng2008@yahoo.cn

Received: 5 March 2013 / *Accepted:* 29 March 2013 / *Published:* 1 May 2013

$LiMnPO_4$ nanoparticles were prepared by a citric acid assisted sol-gel method. The citric acid acts as both a chelating agent in the precursor synthesis and a carbon source in the following calcination. The effects of citric acid content on the structure, morphology and electrochemical performance of $LiMnPO_4$ material were investigated. Higher citric acid content facilitates preparing the material with uniform nanoparticles and multilayer structure, which is benefit for the electrochemical property of $LiMnPO_4$. The optimized materials were obtained with the ratio of citric acid to manganese is 2.0, which exhibits best electrochemical performance among the samples.

Keywords: $LiMnPO_4$; electrochemical performance; citric acid; sol-gel method

1. INTRODUCTION

$LiCoO_2$ has been widely used as the cathode material for commercial lithium ion batteries in the portable applications. However, the disadvantages of high cost, limited discharge capability and toxicity have blocked its further applications in high power and price-sensitive field. Therefore, many efforts have been made to find alternative cathode materials to $LiCoO_2$ [1]. Among various cathode materials, the phosphate-based materials have been considered as the most promising alternative material. Because of the strong covalent P-O bond, the phosphate-based materials exhibit better thermal stability and facilitate a stable operation of the battery especially at elevated temperatures [2-4]. In the phosphate family, $LiFePO_4$ has received special interest owing to its easy preparation and excellent electrochemical performance. However, the low working voltage (3.4 V vs. Li/Li^+) and low

density of $LiFePO_4$ have inhabited its application [2,5-6]. When replacing Fe by Ni and Co in the olivine structure, the $LiNiPO_4$ and $LiCoPO_4$ obtain higher working voltage of 4.8 V and 5.1 V respectively. However, the decomposition of electrolyte tends to appear under such high voltage [7]. A reasonable working voltage of 4.1 V is obtained as replacing Fe by Mn in the lithium iron phosphate, and $LiMnPO_4$ obtains a high energy density of 684 $Wh \cdot kg^{-1}$. However, the poor conductivity of $LiMnPO_4$ makes its practical capacity much lower than the theoretical capacity and inhabits its further use in commercial applications [8-9].

In order to improve the electronic conductivity and lithium ion mobility of $LiMnPO_4$, various strategies such as the conductive surface coating, particle size reduction and cations doping have been applied on $LiMnPO_4$ [10]. Zhumabay Bakenov and Izumi Taniguchi synthesized spherical $LiMnPO_4$/C composite by a combination of spray pyrolysis and spray drying, and good rate capacity were obtained at elevated temperature [11]. Y. R. Wang et al prepared $LiMnPO_4$ by solvothermal method, the rod-like nanosize particle obtained improved lithium ion diffusion coefficient [12]. J. F. Ni and L. J. Gao synthesized Cu doped $LiMnPO_4$ via hydrothermal route, and improved electrochemical property was obtained as the doping amount is 2 wt.%. Although all these strategies make positive effects on $LiMnPO_4$, the preparation processes are complex and the electrochemical performance of $LiMnPO_4$ is not satisfactory until now [13-14].

In this paper, a simple sol-gel method based on citric acid is employed to synthesize $LiMnPO_4$. Citric acid acts as both a chelating reagent and a carbon source in the synthetic process. The effects of citric acid content on the structure, morphology and electrochemical property of $LiMnPO_4$ are discussed.

2. EXPERIMENTS

2.1 Sample preparation

The $LiMnPO_4$/C composite was prepared by a sol–gel method. The starting materials were analytically pure $LiOH \cdot H_2O$, $Mn(CH_3COO)_2 \cdot 4H_2O$ and $NH_4H_2PO_4$. Stoichiometric amounts of the starting materials were firstly dissolved in distilled water under magnetic stirring. To this solution, an aqueous solution of citric acid with desired content was slowly added under magnetic stirring. The resulting mixture was kept stirring at 80 °C until a wet gel was formed. The wet gel was dried at 100 °C over night to form a dry gel. The dry gel was grounded and calcinations under 600 ^oC in flowing argon.

2.2 Measurements

Powder X-ray diffraction (XRD, Bruke D8) employing Cu Kα radiation was used to identify the crystalline phase of the materials. The surface morphology was observed with a scanning electron microscope (SEM, HITACHI S-4700). The surface layer was observed with a transmission electron microscope (TEM, JEOS-2010). The composite electrode was made from a mixture of the prepared

sample, acetylene black, and Polyvinylidene Fluoride (PVdF) in a weight ratio of 80:10:10. Galvanostatic charge-discharge measurements were performed in a potential range of 2.5-4.5 V.

3. RESULTS AND DISCUSSION

In our study, we investigate the effects of citric acid content on the morphology, structure and electrochemical property of $LiMnPO_4$. Fixing the other preparation conditions, the ratio of citric acid to manganese acetate varies to 2/3, 1 and 2, and as prepared materials are marked as LMP-2/3, LMP-1 and LMP-2 respectively. Figure 1 (a)-(c) shows the SEM images of the samples with different citric acid content. Large aggregates of about 0.5~1 μm are observed for all the samples and they are all composed of the small primary particles. When the ratio of citric acid to manganese is 2/3, random shape and broad particle size distribution of 100~300 nm are observed for LMP-2/3. As the citric acid content increases, smaller primary particles with more uniform particle size distribution are observed. As the ratio increases to 2, the LMP-2 exhibits uniform particles with the size of 50-100 nm.

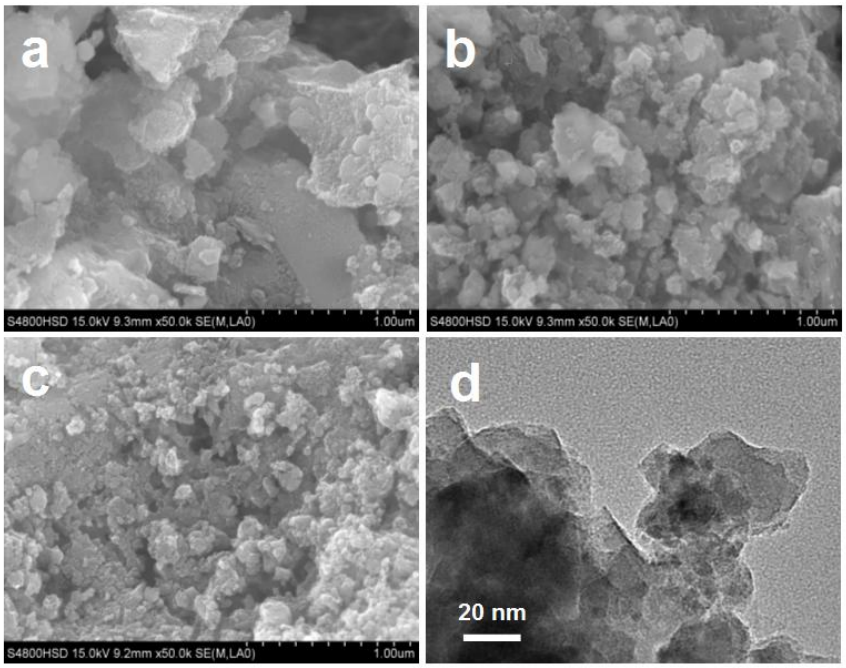

Figure 1. SEM and TEM images of the samples with different citric acid content. The ratio of citric acid to manganese acetate is 2/3 (a), 1 (b) and 2 (c). The TEM image of the LMP-2 sample is shown in Figure 1 (d).

The detailed morphological characteristics of LMP-2 were further clarified by high-resolution transmission electronic microscopy, and the results are shown in Figure 1 (d). Small particles with the size of about 50 nm are observed in the HRTEM figure, which is coincided with the SEM results. A thin surface layer is observed on the surface of the particle, which builds the multilayer of the material.

The surface layer on the particles can be attributed to the residual carbon, which builds a high conductive layer for $LiMnPO_4$ and facilitates its electronic and ion mobility.

The XRD patterns of all the samples are shown in Figure 2. All diffraction peaks of the samples can be indexed to orthorhombic structure in space group *Pnma* (JPDS 33-0804) without the formation of other impurities. No diffraction peaks corresponding to residual carbon are detected, indicating its amorphous nature. As the citric acid content increases, the intensity of the peaks decreases correspondingly, indicating the smaller particle size and lower crystallinity of material. Based on above results, higher citric acid content facilitates to produce uniform particles with smaller particle size, which is benefit for the electrochemical property of the $LiMnPO_4$ material.

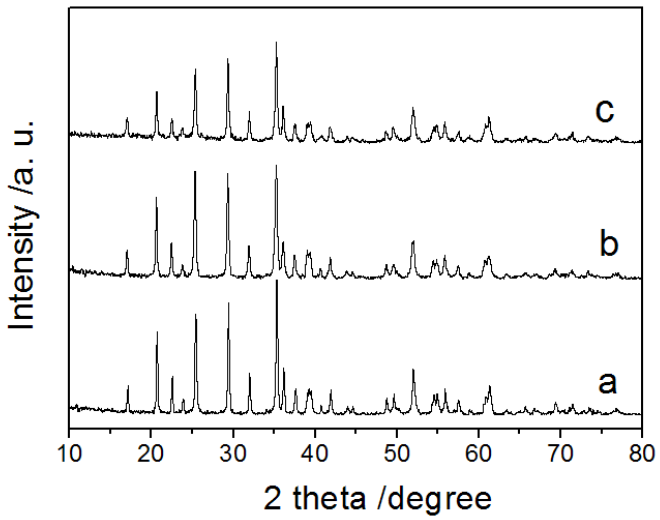

Figure 2. XRD patterns of the samples with different citric acid content. The ratio of citric acid to manganese acetate is 2/3 (a), 1 (b) and 2 (c).

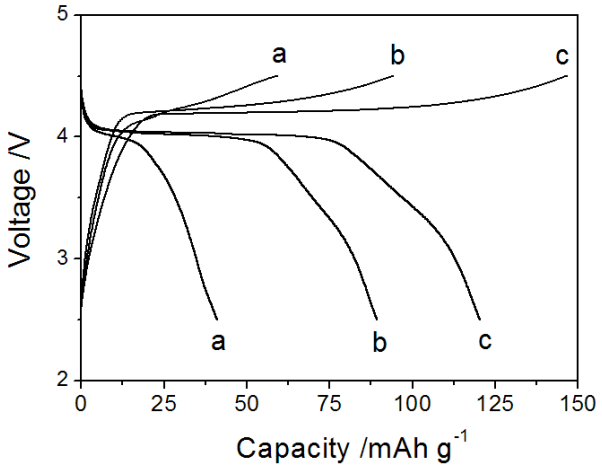

Figure 3. The charge/discharge curves of the LMP-2/3 (a), LMP-1 (b) and LMP-2(c) samples with different citric acid content at the current density of C/20 in the voltage range of 2.5-4.5 V.

The electrochemical characteristics of the samples with different citric acid content are shown in Figure 3 and 4. Figure 3 shows the typical charge/discharge curves of the samples at the current density of C/20 in the voltage range 2.5-4.5 V. All the materials present a reversible voltage plateau around 4.1 V, corresponding to the redox couple of Mn^{3+}/Mn^{2+}. As the citric acid content increases, the discharge capacity increases correspondingly. Among the samples, the highest charge/discharge capacities are obtained for the LMP-2. Compared with the previous report [15, 16], the better electrochemical performance was obtained in our study, which is associated with the nanosize particles of the samples.

The differential capacities of all the samples were calculated and the results are shown in Figure 4. The dQ/dV vs. V curve provides information similar to that of cyclic voltammograms. The oxidation/reduction peaks in the curves correspond to the charge/discharge plateaus in the charge/discharge curves. As citric acid content increases, the redox peaks become sharper and the difference between the redox peaks become larger. The LMP-2 exhibits the sharpest peaks and the lowest difference, which indicates its lowest electrochemical polarization among the samples.

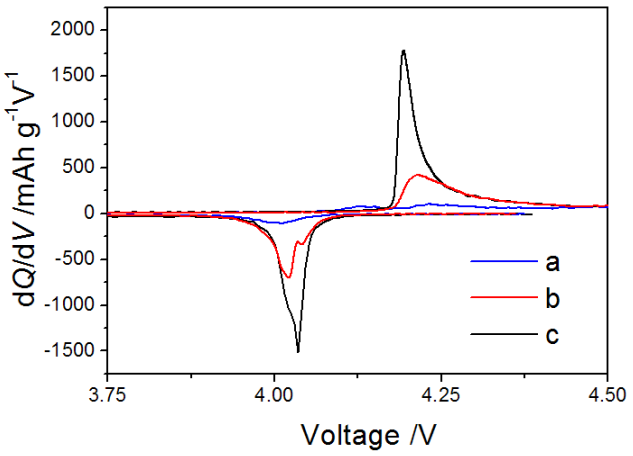

Figure 4. The differential capacities of the LMP-2/3 (a), LMP-1 (b) and LMP-2(c) samples with different citric acid content.

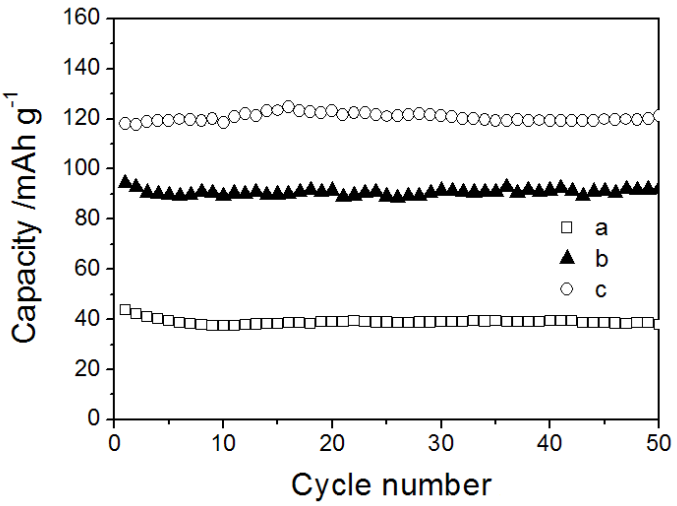

Figure 5. Cycle performance of the LMP-2/3 (a), LMP-1 (b) and LMP-2(c) samples with different citric acid content.

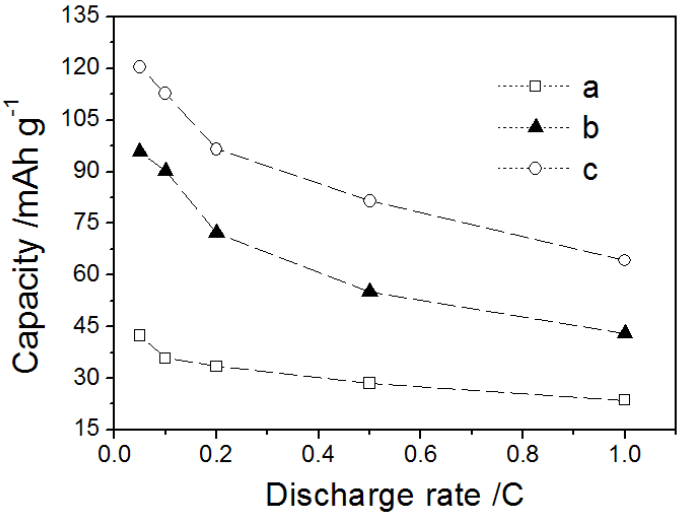

Figure 6. The rate capability of the LMP-2/3 (a), LMP-1 (b) and LMP-2(c) samples with different citric acid content.

The cycle performance and rate capability of all the samples were shown in Figure 5 and 6. As citric acid content increases, both the cycle stability and the rate capability increase correspondingly. The LMP-2 material obtains the highest capacities at all the current densities and the highest capacity retention among the samples. The result indicates that higher citric acid content is benefit for the electrochemical property of $LiMnPO_4$. The improved property of LMP-2 is associated with its uniform nanoparticles and multilayer structure induced by citric acid in the synthetic process. Therefore, the optimized citric acid content in our work is determined with the ratio of citric acid to manganese is 2.0.

4. CONCLUSIONS

$LiMnPO_4$ composite material was synthesized by a sol-gel route based on citric acid, which acts as both a chelating agent and a carbon source. The citric acid contents were varied to optimize the physical and electrochemical properties of prepared $LiMnPO_4$. The structural, morphological and electrochemical properties of the prepared material were characterized by XRD, SEM, TEM and galvanostatic charge/discharge cycling. The material prepared with the ratio of citric acid to manganese is 2.0 exhibits the highest capacity, lowest polarization and best cycling stability among the samples. It can be attributed to the nanoparitlces, conductive layer and good crystal induced by citric acid in the synthetic process.

ACKNOWLEGEMENTS
This work is supported by the National Natural Science Foundation of China (No. 21001036, 50902041) and Fundamental Research Funds for the Central Universities (HEUCF201310011).

References

1. S. Zhang, Q. Wu, C. Deng, F. L. Liu, M. Zhang, F. L. Meng, H. Gao, *J. Power Sources*, 218 (2012) 56.

2. A. K. Padhi, K. S. Nanjundaswamy, J. B. Goodenough, *J. Electrochem. Soc.*, 114 (1997) 1188.
3. A. K. Padhi, K. S. Nanjundaswamy, C. Masquelier, S. Okada, J. B. Goodenough, *J. Electrochem. Soc.*, 114 (1997) 1609.
4. C. Deng, S. Zhang, S. Y. Yang, B. L. Fu, L. Ma. *J. Power Sources*, 196(2011)386.
5. A. Yamada, S. C. Chung, K. Himnokuma, *J. Electrochem. Soc.*, 148 (2001) A224.
6. H. Huang, S. C. Yin, L. F. Nazar, *Electrochem. Solid-State Lett.* 4 (2001) A170.
7. J. Wolfenstine, J. Allen, *J. Power Sources*, 136 (2004) 150.
8. S. Franger, C. Bourbon, F. L. Cras, *J. Electrochem. Soc.*, 151 (2004) A1024.
9. M. Yonemura, A. Yamada, Y. Takei, N. Sonoyama, R. Kanno, *J. Electrochem. Soc.*, 151 (2004) A1352.
10. T. N. L. Doan, Z. Bakenov, J. Taniguchi, *Adv. Power Technol.*, 21 (2010) 187.
11. Z. Bakenov, I. Taniguchi, *Mater. Res. Bull.*, 46 (2011) 1311.
12. Y. R. Wang, Y. F. Yang, Y. B. Yang, H. X. Shao, *Solid State Commun.*, 150 (2010) 81.
13. C. Delacourt, L. Laffont, R. Bouchet, C. Wurm, J. B. Leriche, M. Morcrette, J. M. Tarascon, C. Masquelier, *J. Electrochem. Soc.*, 152 (2005) A913.
14. M. Yonemura, A. Yamada, Y. Takei, N. Sonoyama, R. Kanno, *J. Electrochem. Soc.*, 151 (2004) A1352.
15. L. Wang, W. T. Sun, X. M. He, J. J. Li, C. Y. Jiang, *Int. J. Electrochem. Sci*, 6 (2011) 2022-2039.
16. H. S. Fang, E. Dai, K. Yang, B. Yang, Y. Yao, W. Ma, Y. Dai, *Int. J. Electrochem. Sci*, 7 (2011) 11827-11833.